# Geology of the Melas Chasma landing site for the Mars Exploration Rover mission

Catherine M. Weitz,[1,2] Timothy J. Parker,[3] Mark H. Bulmer,[4] F. Scott Anderson,[5] and John A. Grant[6]

Received 3 December 2002; revised 12 June 2003; accepted 9 July 2003; published 22 October 2003.

[1] The Melas Chasma landing site was considered a high-priority site for the Mars Exploration Rover (MER) mission because of the opportunity to land on and study potential layered sedimentary deposits. Though no longer considered a candidate site because of safety concerns, the site remains a scientifically interesting area that provides insight into the geologic history of Valles Marineris. Within the landing ellipse are dunes, landslide material, and unusual blocky deposits. The blocky deposits are composed of rounded blocks, some of which have meter-scale layering, and they show evidence of ductile deformation, including bending and distortion of coherent blocks around each other. The morphologic characteristics of the blocks are unique, and they appear to have no terrestrial analogue. However, the gross morphology of these blocky deposits and their superposition on adjacent wallrock is consistent with the blocks having been transported downslope. Given the existence of other large mass failures in the area, we propose the blocky deposits may also have originated from mass movement events. The size of the blocks coupled with the distances they traveled indicates high mobility. The distances the blocks were transported and their rounded, irregular shapes suggest either water in the source material or deposition in a subaqueous environment. The source for the main blocky deposit inside the landing ellipse is considered to be the wallrock to the south, while the other two blocky deposits have source regions along the northern canyon walls. The southern wallrock of Melas Chasma contains numerous valleys not seen elsewhere in Valles Marineris. The identification of valley networks along the southern wallrock suggests that a source of water existed below the surface of the plateau and produced the valleys after intersecting the edge of the exposed canyon walls. *INDEX TERMS:* 6225 Planetology: Solar System Objects: Mars; 5499 Planetology: Solid Surface Planets: General or miscellaneous; 5470 Planetology: Solid Surface Planets: Surface materials and properties; 5415 Planetology: Solid Surface Planets: Erosion and weathering; *KEYWORDS:* Valles Marineris, Melas Chasma, MER, landslides, valleys, mass wasting

**Citation:** Weitz, C. M., T. J. Parker, M. H. Bulmer, F. S. Anderson, and J. A. Grant, Geology of the Melas Chasma landing site for the Mars Exploration Rover mission, *J. Geophys. Res.*, *108*(E12), 8082, doi:10.1029/2002JE002022, 2003.

## 1. Introduction

[2] Melas was initially selected as a high-priority landing site for the Mars Exploration Rover (MER) mission at the First Landing Site Workshop held in January of 2001 [*Weitz et al.*, 2001a]. The site was considered scientifically compelling because of layered deposits found within the landing ellipse. In addition, the site would have provided vistas of the canyon walls in the distance, which was considered to be interesting both for scientific reasons and for public engagement. Melas was removed as a landing site at the end of the Third Landing Site workshop in March of 2002 for several reasons. In particular, mesoscale wind models predicted high winds and wind shear above the site that exceeded the engineering safety criteria required during the Entry-Descent-Landing Phase [*Rafkin and Michaels*, 2003; *Toigo and Richardson*, 2003; *Kass et al.*, 2003]. In addition, slopes derived from MOC stereo images by *Kirk et al.* [2002] and from MOLA altimetry [*Anderson et al.*, 2003] indicated that there were locations that exceeded the 15° slope limit for Entry-Descent-Landing safety. Other concerns about the landing site in Melas included the high percentage of dune fields in the northeast and southwest of the ellipse. Although it is no longer a possible MER landing site, the Melas Chasma site remains a scientifically interesting area that provides insight into the geologic history of Valles Marineris.

[1]Planetary Science Institute, Tucson, Arizona, USA.
[2]Also at NASA Headquarters, Washington, DC, USA.
[3]Jet Propulsion Laboratory, Pasadena, California, USA.
[4]Joint Center for Earth Systems Technology, University of Maryland, Baltimore, Maryland, USA.
[5]University of Hawai'i at Manoa, Hawai'i Institute of Geophysics and Planetology, Honolulu, Hawaii, USA.
[6]Center for Earth and Planetary Studies, National Air and Space Museum, Smithsonian Institution, Washington, DC, USA.


0148-0227/03/2002JE002022$09.00

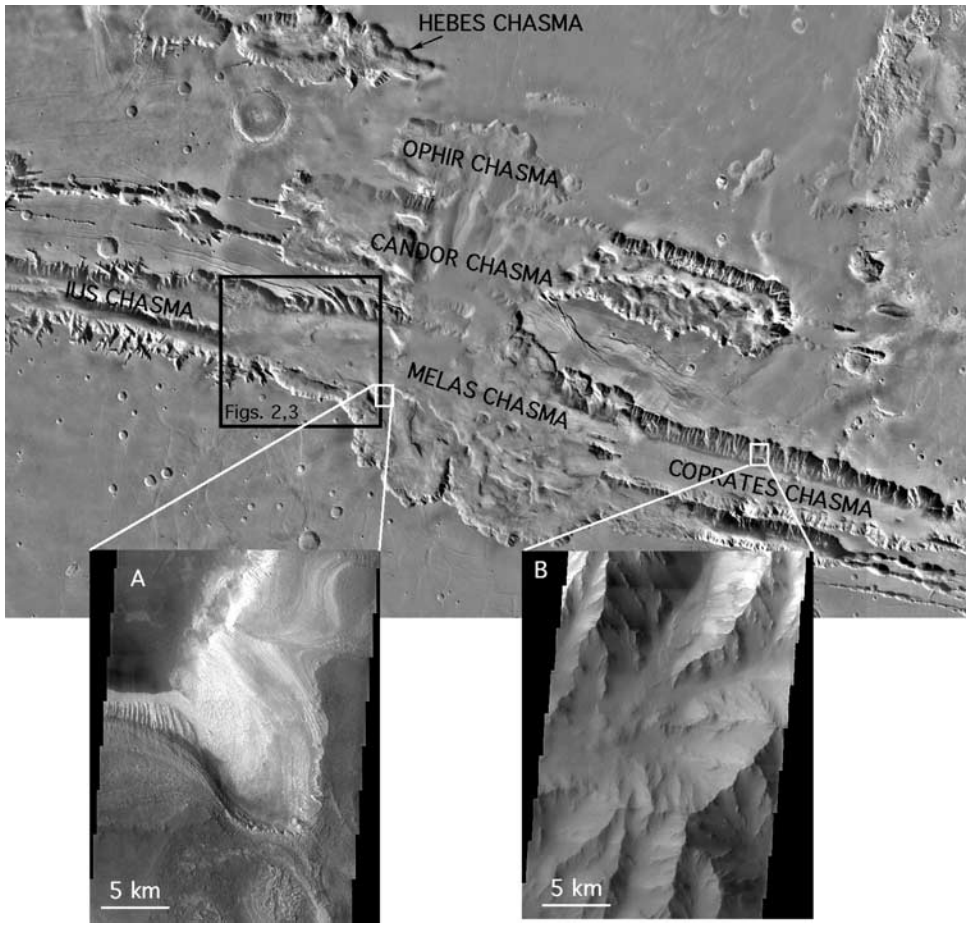


**Figure 1.** Viking MDIM of central Valles Marineris. Black box represents the region studied in detail for this paper and the location of Figures 2 and 3. (A) Blowup of interior layered deposits in Melas Chasma showing layering, terraces, and fluting. Portion of THEMIS visible image V20030512. (B) Blowup of canyon walls in Coprates Chasma, illustrating the typical spur and gully morphology characteristic of the wallrock. Portion of THEMIS visible image V01838002.

[3] Because the Melas Chasma landing site was a high priority ellipse for over a year, there are a significant number of MOC images that were taken of this location. Thus far through Extended Mission E14, there are 30 narrow angle images within the ellipse and several others outside the ellipse that target the surrounding terrain. Approximately 50% of the ellipse has been imaged at a resolution of <6 meter/pixel. A significant portion of the ellipse has also been imaged by THEMIS in the visible and thermal infrared. The THEMIS thermal infrared data sets at 100 meter/pixel resolution can be used for morphologic, compositional, and thermophysical identification of units. The THEMIS visible images at 18 m/pixel provide context for the narrow angle MOC images at a more practical scale than the lower resolution Viking images. Three pairs of MOC images have sufficient overlap to produce stereo images and anaglyphs to aid in the interpretation of slopes and topography at higher spatial resolution than provided by MOLA data. Digital Elevation Models (DEMs) have also been produced from these stereo pairs and were analyzed by *Kirk et al.* [2002]. MOLA data have been used to determine slopes, thickness, and roughness of the deposits and enable a calculation of their volumes at the Melas location. We have analyzed individual MOLA profiles that were taken along MOC narrow angle images. These coexisting data sets allow us to identify topographic variations associated with the MOC imagery that could not be interpreted from the images themselves.

[4] For this paper, we report on the geology of the landing ellipse and the surrounding terrain (Figure 1) using available data sets from Viking, Mars Global Surveyor, and Mars Odyssey. We have characterized, mapped, and proposed origins for the different geologic units in this region. We also discuss what questions could be addressed had this site been selected for MER or should a future rover be sent to this site.

## 2. Background on Valles Marineris Geology

### 2.1. Troughs and Landslides

[5] The troughs of Valles Marineris are thought to have formed by subsurface removal of groundwater or tectonic extension [*Schultz*, 1990, 1991, 1995, 1997; *Tanaka*, 1997; *Mège and Masson*, 1996a, 1996b; *Peulvast and Masson*, 1993a, 1993b; *Lucchitta et al.*, 1992]. Two main competing interpretations have developed for the formation of Valles Marineris: (1) tectonic subsidence, or (2) fluvial or subsurface withdrawal. As reviewed by *Anderson and Grimm* [1998], features supporting a tectonic origin include (1) gra-

ben-like form and interior fault scarps of the rectangular troughs Coprates, Ius, and East Candor [*Schultz*, 1991; *Peulvast and Masson*, 1993a, 1993b]; (2) downdropped Hesperian-age floor [*Blasius et al.*, 1977; *Lucchitta and Bertolini*, 1989; *Schultz*, 1990, 1991; *Lucchitta et al.*, 1992; *Tanaka*, 1997]; (3) long, linear form of the trough system, radial to Tharsis and in agreement with stress predictions [*Banerdt et al.*, 1992]; and (4) parallelism and comparatively regular spacing of the troughs, an observation used by *Anderson and Grimm* [1998] to constrain rift models. Abundant small faults and graben are apparent in Valles Marineris [*Schultz*, 1991; *Lucchitta et al.*, 1992], while extension at Noctis Labyrinthus appears to have been controlled by preexisting planes of weakness with different orientations [*Lucchitta et al.*, 1992]. These observations support the hypothesis that the Valles Marineris system initially formed through crustal extension. There is abundant evidence for faulting in the region, oriented parallel to the canyons, so a certain amount of extension is possible.

[6] However, the canyons also commonly exhibit amphitheater terminations, particularly the closed systems, such as Hebes Chasma, with only relatively modest-scale faulting extending across the plateau surface at either end. This observation suggests that the canyons must also be enlarged by collapse due to removal of massive amounts of bedrock. *Tanaka and MacKinnon* [2000] proposed that portions of Valles Marineris could be the result of subsurface collapse and erosion by groundwater.

[7] Evidence for fluvial erosion and subsurface withdrawal [*Lucchitta et al.*, 1992; *Peulvast and Masson*, 1993a; *Schultz*, 1997; *Tanaka*, 1997; *Tanaka and MacKinnon*, 2000] includes (1) outflow channels, which appear to be the source of catastrophic floods, emanate from the canyons; (2) the layered appearance of the interior deposits, supporting a sedimentary origin in lakes; (3) the large depth of pit craters and closed troughs; and (4) the extension of gravitational anomalies associated with the Valles Marineris northward under the outflow channels [*Zuber et al.*, 2000]. Hebes Chasma in particular is difficult to explain as a graben and is instead suggestive of collapse or removal of groundwater or ice [*Spencer and Fanale*, 1990].

[8] Landslides are common on the floors of Valles Marineris. Their morphologies have been examined in detail in an attempt to determine if their emplacement involved an interstitial fluid or occurred in a subaqueous environment [*Lucchitta*, 1987; *McEwen*, 1989; *Shaller*, 1991]. The large landslides on Mars have similar attributes to terrestrial rock avalanches [e.g., *Voight and Pariseau*, 1978] and rockslides [*Heim*, 1932; *Shreve*, 1966; *Varnes*, 1978], including longitudinal grooves and debris lobes. Initially, definitive diagnosis was hindered by the limitations of Viking Orbiter images. Significant improvements in imaging data from MOC and in topography from MOLA, as well as advances in understanding of terrestrial landslides have reawakened the debate [e.g., *Bulmer et al.*, 2002, 2003]. On the basis of these new data sets, it is apparent that landsliding has been a significant process in the modification of the Valles Marineris.

### 2.2. Interior Layered Deposits

[9] The interior layered deposits (ILDs) of Valles Marineris were first identified in the Mariner 9 images [*McCauley*, 1978] yet their origin still remains a mystery. The ILDs consist of large mounds or mesas concentrated toward the interiors of the canyons. The deposits can be as high as the adjacent wallrock and hundreds of kilometers in length. The original layering seen in both Mariner and Viking images was later attributed in MOC images to topographically flat areas along the sides of the units where dust and debris had accumulated to produce darker layers [*Weitz et al.*, 2001b]. However, even finer, meter-scale layering is visible in MOC and THEMIS visible images and appears to represent actual discontinuities in the deposits, rather than material covering them.

[10] The deposits have been studied in detail by numerous investigators because they might reveal important insights into the geologic history of Mars. The ILDs have been proposed as (1) sedimentary deposits formed in lakes [*McCauley*, 1978; *Nedell et al.*, 1987; *Komatsu et al.*, 1993; *Weitz and Parker*, 2000; *Malin and Edgett*, 2000]; (2) mass wasted material from the walls [*Nedell et al.*, 1987; *Lucchitta et al.*, 1994]; (3) remnants of the wall rock [*Malin*, 1976]; (4) carbonate deposits [*Spencer and Croft*, 1986; *Spencer and Fanale*, 1990]; (5) aeolian deposits [*Peterson*, 1981; *Nedell et al.*, 1987]; and (6) volcanic deposits [*Peterson*, 1981; *Lucchitta*, 1990; *Lucchitta et al.*, 1994; *Weitz*, 1999; *Chapman and Lucchitta*, 2000; *Chapman and Tanaka*, 2001; *Chapman*, 2001].

[11] The ILDs are generally thought to span several ages from Hesperian to Amazonian based upon stratigraphic relationships with other units in the canyons and also on crater counts, with most of the deposition concurrent with formation of the troughs [*Lucchitta*, 1990]. Later episodes of tectonism and erosion are thought to have caused the ILDs to remain as mesas inside the troughs. *Lucchitta* [1990] reported three younger units of light-colored ILDs that may be Amazonian in age. In contrast, *Schultz* [1997] proposed that there may be a few examples where the ILDs predate the troughs and now appear as perched remnants. *Malin and Edgett* [2000] interpret the ILDs as sedimentary deposits that formed in old impact craters, which subsequently were buried and later exposed during formation of Valles Marineris. However, as previously shown in Viking images [*Komatsu et al.*, 1993; *Schultz*, 1991; *Lucchitta*, 1990] and also supported by MOC data [*Weitz et al.*, 2001b; *Lucchitta*, 2001], the ILDs are superimposed upon the chaotic terrain and floor material in several of the canyons, which supports a younger age for the ILDs relative to the formation of Valles Marineris. Consequently, whatever the source for the ILDs, most of their deposition appears to have occurred after formation of much of the Valles Marineris system.

[12] The ILDs are likely composed of different material than the canyon wallrock because they have fluting or yardangs along their sides (Figure 1a), compared to the typical spurs of bedrock separated by talus chutes seen on the wallrocks (Figure 1b). This different style of erosion between the two units most likely reflects variations in composition or induration. MOC images of the wallrock indicate prevalent layering throughout the height of the rockface, which several researchers suggest supports a volcanic origin due to similarities with layering seen in volcanic flood basalts [*McEwen et al.*, 1999]. *Caruso and*

*Schultz* [2000] used MOLA-derived slopes to infer a sedimentary rock for the ILDs and an igneous rock for the wallrock. *Malin and Edgett* [2000] suggested that the fine-scale, rhythmic layering seen in the ILDs, as well as other layered deposits identified in impact craters around the equator (i.e., Becquerel, Gale), supports a sedimentary origin for Martian layered deposits. Investigators have noted that the deposits in each canyon have distinct morphologies suggesting different formational histories [*Komatsu et al.*, 1993].

[13] The high-resolution MOC imagery reveals that the layering in the ILDs can be fine-scale, with layers visible at the resolution of a few meters per pixel. Deposition of volcanic ash or aeolian dust from the atmosphere into lakes within Valles Marineris is a plausible explanation for producing similar layers within each chasmatae, but the restriction of the ILDs to only certain portions of the chasmatae would still need to be elucidated. *Malin and Edgett* [2000] argue against a pyroclastic ash origin because the ILDs have thicker beds compared to the centimeter-size deposits on Earth, and there is no thinning of the ash with distance from any proposed vents. In addition, the deposits are confined to topographic basins yet ash should be deposited radially outward from a source (assuming no wind) at all localities irregardless of height. The lack of any large calderas inside Valles Marineris that could have produced such large quantities of pyroclastic ash also argues against this origin.

[14] The ILDs could be stacks of aeolian deposits, a hypotheses proposed by *Malin and Edgett* [2000] for the layered deposits seen in Valles Marineris and elsewhere on Mars. These authors proposed that in the Martian past, conditions were more favorable to suspend and transport greater amounts of material, either as aeolian dust or volcanic ash. Many morphologic features in the ILDs resemble tuyas produced on Earth by subglacial eruptions [*Chapman and Tanaka*, 2001; *Chapman and Lucchitta*, 2000]. Several investigators have proposed that the ILDs could have formed in standing bodies of water. *McCauley* [1978] proposed that the layering and lateral continuity of the deposits could best be explained by deposition within lakes. *Nedell et al.* [1987] investigated how aeolian debris could accumulate on ice-covered lakes in the troughs and then by Rayleigh-Taylor instability falter through the ice to form the ILDs. The height of the ILDs in some canyons, like Hebes Chasma, is comparable to the adjacent canyon wall, which has been used to argue against a lacustrine origin for the deposits [*Chapman and Tanaka*, 2001]. Consequently, if the ILDs are lacustrine sediments then the lake must have superceded the canyon walls in height and have been greater in aerial extent than the canyons.

[15] Spectral data from Viking [*Geissler et al.*, 1993] and the more recent Phobos II ISM imaging spectrometer [*Murchie et al.*, 1992, 2000] reveal variable mafic mineralogy and different states of hydration in the canyons and ILDs. TES data may also reveal distinct geologic units within Valles Marineris [*Gaddis and Titus*, 2000]. In fact, TES results indicate that there are a few small areas of crystalline hematite associated with the ILDs of Ophir, Candor, and Melas Chasmatae [*Christensen et al.*, 2000]. A similar but much larger region of crystalline hematite has been identified in Sinus Meridiani and interpreted as either a chemical precipitate from Fe-rich water [*Christensen et al.*, 2000] or a volcanic deposit [*Arvidson et al.*, 2003].

## 3. Geology and Physical Properties of the Melas Landing Site

[16] The center location of the Melas landing ellipse for both MER-A and MER-B is at 8.8°S, 77.8°W, on the floor of western Melas Chasma and eastern Ius Chasma (Figures 1 and 2). The size of the ellipse is 105 × 20 km. Previous mapping of the area from Viking data by *Witbeck et al.* [1991] has most of the landing site comprised of a rough floor material consisting of rubble and debris that formed by erosion from the canyons walls. This same unit is also mapped throughout the floor of Valles Marineris.

[17] Our geological interpretation of the units within Melas is predominantly based upon the MOC narrow angle and THEMIS thermal infrared images, with additional understanding provided by Viking images and MOLA altimetry. When referring to units as "bright" or "dark", it should be understood that these are relative terms because the MOC images are not radiometrically corrected. We have mapped three main geologic units within the landing ellipse (Figure 3): [1] blocky deposits typically consisting of brighter, oval blocks in a darker matrix (BD and $BD_3$); [2] dark sand sheets (SS) and sand dunes (SD); and [3] a landslide deposit emanating from the northwest ($LS_2$). To the north of the ellipse we have mapped another blocky deposit, $BD_2$, predominantly based upon THEMIS thermal infrared images. There is no MOC coverage of $BD_2$ to compare its meter-scale geology to units BD and $BD_3$, but the thermophysical properties and morphology seen from THEMIS thermal infrared images suggest it has the same characteristics of the other blocky deposits.

### 3.1. Physical Properties of the Melas Geologic Units

[18] There is a strong correlation between thermal inertia and the outcroppings of bright blocks in units BD, $BD_2$, and $BD_3$ on the floor of Melas. Thermal inertias derived from TES [*Mellon et al.*, 2000] have values around 500–550 $Jm^{-2}K^{-1}s^{-1/2}$ for unit BD inside the ellipse. The floor of Melas is covered by sand dunes (SD) and has values between 250 and 370 $Jm^{-2}K^{-1}s^{-1/2}$. Based upon the thermal inertias, BD most likely represents a relatively dust-free surface composed of cemented, competent material. The albedo for the Melas ellipse ranges from 0.13–0.17, which also supports an area with little dust [*Golombek et al.*, 2003]. A detailed study of the TES and THEMIS data for the Melas site was performed by *Pelkey and Jakosky* [2003]. Thermophysical units are visible in the landing ellipse and correlate well with geologic features that can be mapped from visible images. In general, the Melas canyon floor has higher thermal inertias and is darker than the adjacent plateau, indicating a rougher and rockier surface [*Pelkey and Jakosky*, 2003].

[19] Figure 4a illustrates daytime thermal infrared images of the Melas site. The blocky deposits BD, $BD_2$, and $BD_3$ are visible as darker, patchy features. A corresponding nighttime thermal infrared mosaic of the

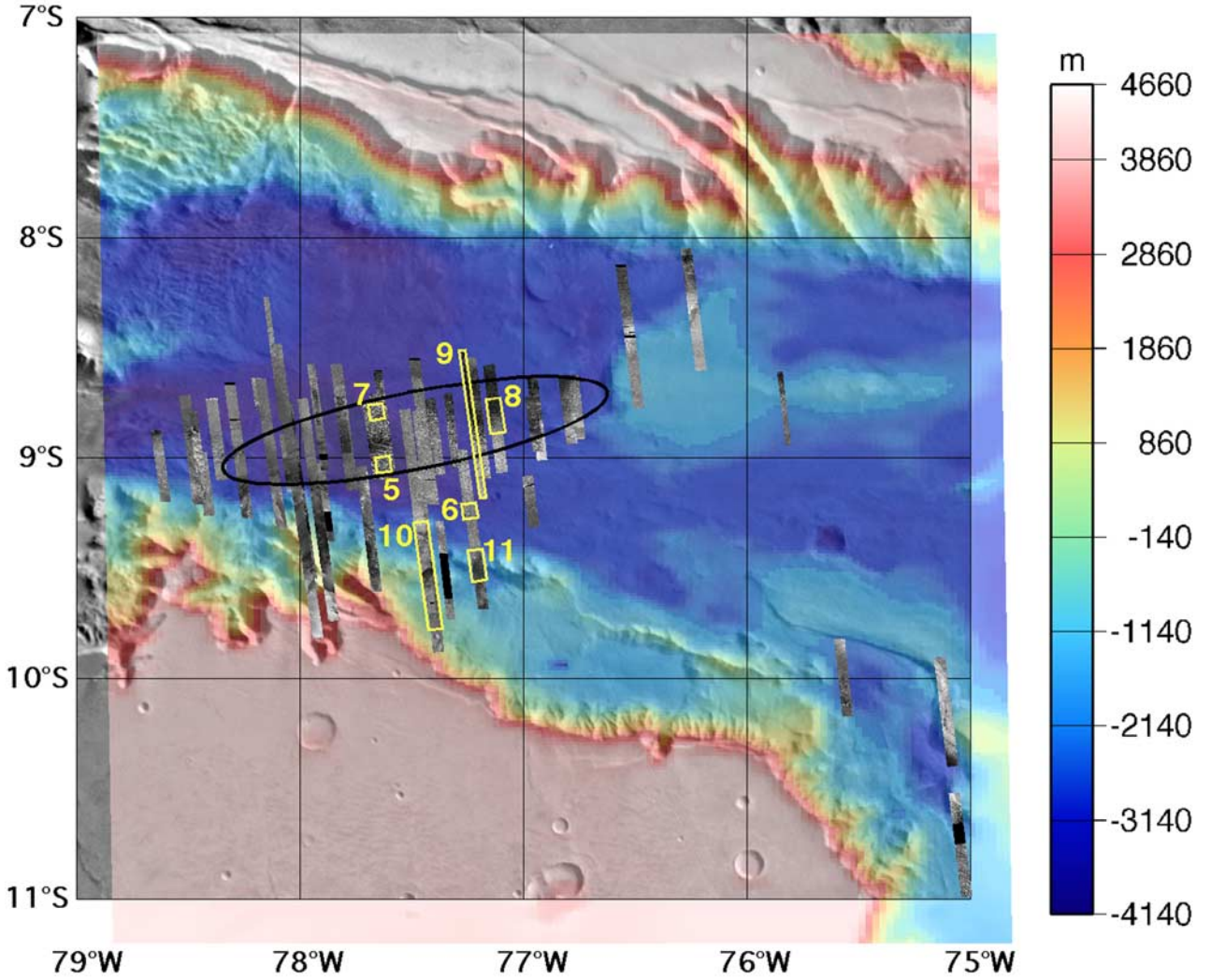


**Figure 2.** Viking MDIM of western Melas Chasma and eastern Ius Chasma with MOLA topography (color) and MOC images (gray strips) superimposed. Dark blue colors on the floor of Melas at the location of the landing ellipse range from −4140 to −2700 m. The location of the proposed MER-B ellipse is shown and it is 105 × 20 km in size. The MER-A ellipse is centered at the same location but is rotated a few degrees counter-clockwise due to the earlier arrival date. The ellipse also rotates slightly depending upon if the spacecraft launches early or late in the launch window. Yellow boxes and numbers refer to later figures in the paper.

ellipse (Figure 4b) shows units BD, $BD_2$ and $BD_3$ to be bright deposits. These thermal infrared properties indicate a dust-free indurated or rocky surface with higher thermal inertias than the surrounding terrain. Longitudinal grooves on landslides $LS_1$, $LS_2$ and $LS_3$ are also seen in both day and night thermal infrared images and have been filled in with dust. The sand dune unit, SD, appears relatively bright in the daytime image and dark in the nighttime image, as would be expected for a dusty or sandy feature with relatively lower thermal inertia. Finally, both the day and nighttime thermal infrared images reveal numerous valleys flowing down the southern wallrock. The valleys are particularly visible in the nighttime infrared image as dark features along the brighter wallrock (Figure 4b). Similar valleys are not seen elsewhere along the canyon walls in Valles Marineris, though the MOC and THEMIS coverage is currently more limited in other parts of the canyon.

### 3.2. Geological Interpretation of the Melas Site and Surrounding Terrain

#### 3.2.1. Blocky Deposits (BD, $BD_2$, and $BD_3$)

[20] Three blocky deposits (BD, $BD_2$, and $BD_3$) have been identified in the region of study. The area of the blocky deposit BD is approximately 1800 $km^2$. Very few craters are visible on the surface of BD, which may be due to (1) a relatively young age; (2) erosion and removal of craters; or (3) burial soon after deposition followed by recent exhumation by the wind. Layering is visible in a few of the MOC images of the blocks (Figure 5), supporting that unit BD emanated or contains material from layered deposits. The blocks are typically oval or have rounded edges. Several of

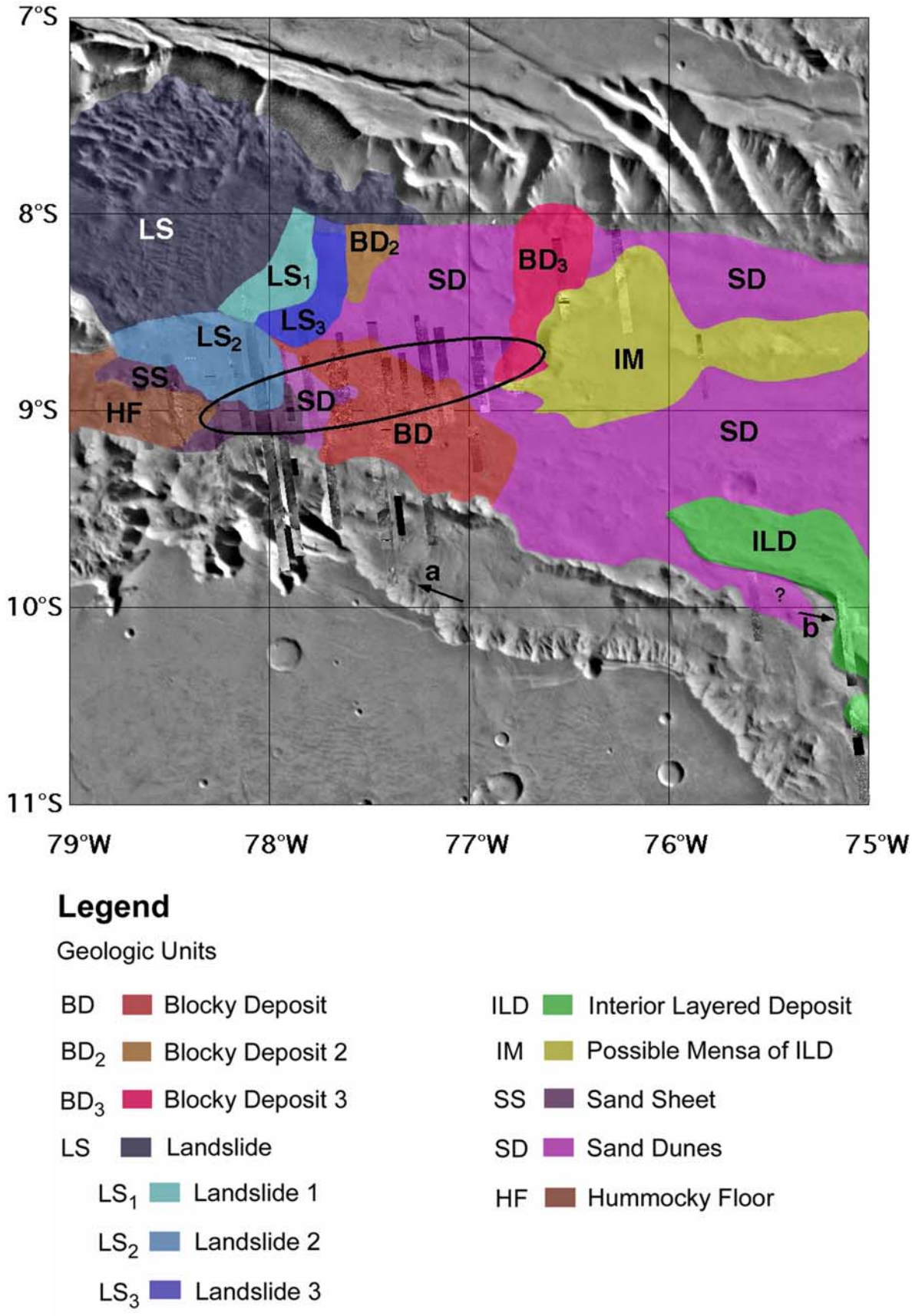


**Figure 3.** Geologic map of the Melas landing site and surrounding terrain. See text for a description of each unit. The two black arrows with lettering show locations of proposed sources for unit BD that are discussed in the paper.

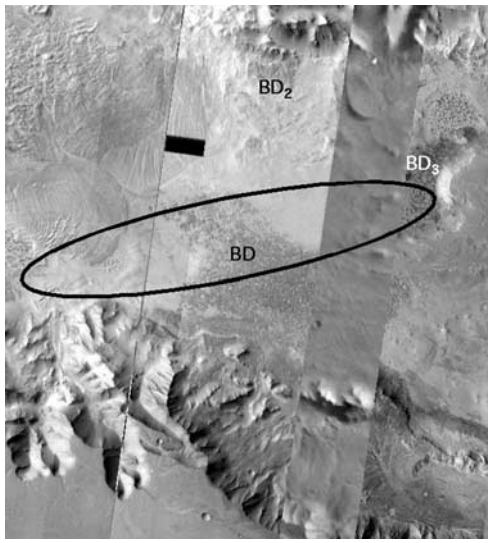


**Figure 4a.** THEMIS daytime thermal infrared images superimposed on a MDIM2 context image. The landing ellipse, which is 105 km long, is shown in black. Units BD, $BD_2$, and $BD_3$ stand out as dark, blocky features in the thermal images. The thermophysical properties of the blocky deposits suggest a rocky, indurated surface with little dust.

the blocks show evidence of ductile deformation where material appears to have flowed around obstacles (Figure 6). A few blocks within BD have fractures that suggest brittle deformation. There is a variation in the brightness of the blocks, with some appearing brighter toward the edges,

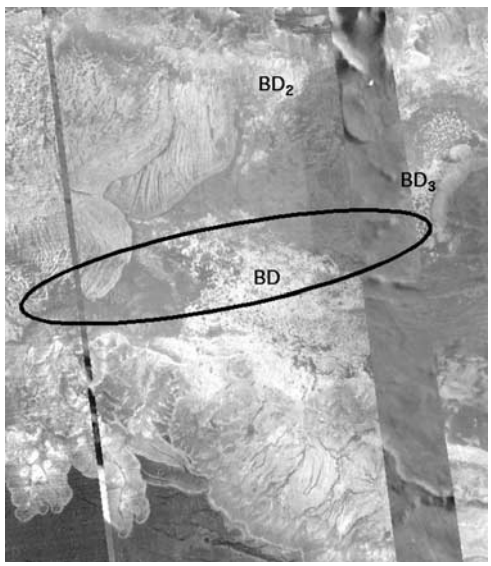


**Figure 4b.** THEMIS nighttime thermal infrared images superimposed on a MDIM2 context image. The blocky deposits, BD, $BD_2$, and $BD_3$ are bright in this image, consistent with rough, dust-free surfaces. The lower part of the figure reveals several dark valleys flowing down the canyon walls. These valleys are likely filled in with dust or fine debris which produces the lower thermal inertia relative to the adjacent wallrock.

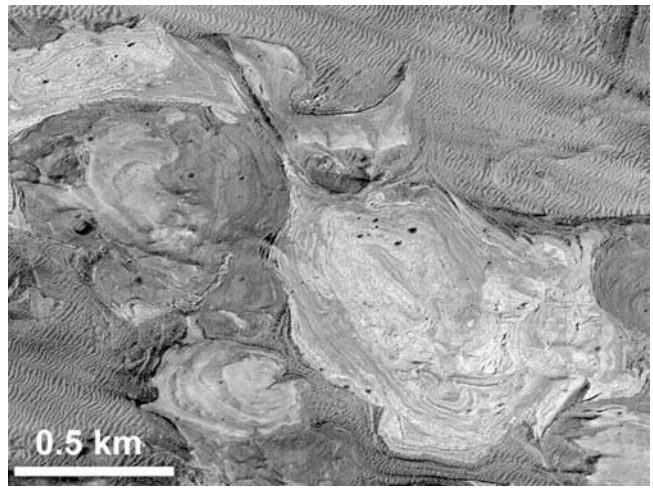


**Figure 5.** Subframe of MOC image E1200720 illustrating layers within the blocks of unit BD. Adjacent to the bright layered blocks is a darker, marbled matrix. Sand dunes fill in topographic lows between the blocks and dark matrix. Small impact craters are also visible and filled with dark debris.

whereas others have variable brightness across individual blocks.

[21] Another smaller unit composed of similar material to BD has been identified to the north of the landing site (Figure 3, $BD_2$). Unit $BD_2$ appears to be partially buried beneath landslide $LS_3$, though this cannot be verified due to lack of MOC coverage. A third blocky deposit, unit $BD_3$, has been mapped in the easternmost portion of the ellipse. It has similar thermophysical properties to unit BD in the THEMIS data, but the blocks appear more angular in shape and there are more dunes obscuring the surface compared to

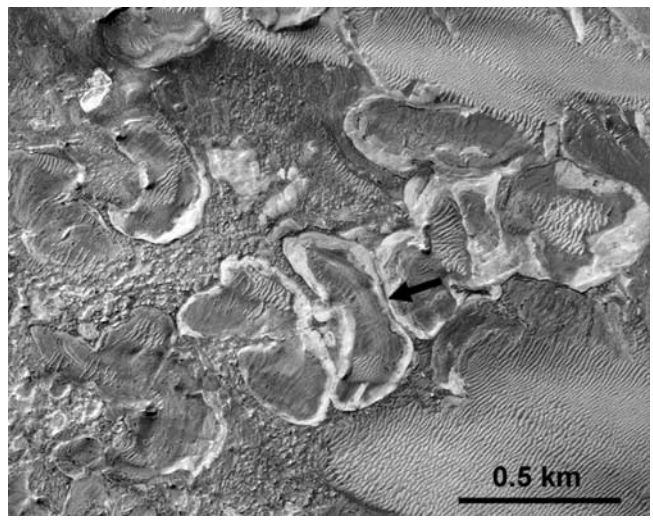


**Figure 6.** Oval-shaped blocks showing possible evidence of flow and plastic deformation. Arrow indicates where two blocks appear to have pushed into each other. The blocks generally have smooth, rounded edges that can either form during deposition or post-emplacement by erosion. These blocks are darker in the centers and have brighter edges. Subframe of MOC image M1900264.


**Figure 7.** This subframe of MOC image E1202596 has a corresponding stereo image (E1200720) that together have been used to infer topographic and stratigraphic relationships. The arrows show a dark mesa-forming unit that is higher than the other units. The mottled blocks have variable reflectances but are at similar heights and appear to have relatively hummocky surfaces. Dunes fill in relative lows between the blocks and dark mesas.

BD. Small patches of $BD_3$ can be seen along the wallrock at higher elevations (~1 km) than the portions along the floor. $BD_2$ also lies along the wallrock slope with elevations approximately 1 km higher to the north than in the southernmost extension of the unit. On the basis of examination of THEMIS data combined with MOLA topography, units BD, $BD_2$, and $BD_3$ appear to be distinct. Both $BD_2$ and $BD_3$ can be traced back to potential escarpments in the wallrock.

[22] Individual blocks inside BD cannot be identified in either the MOLA topography or DEMs. In the stereo images, they appear relatively flat and at the same height as the adjacent darker matrix material. Brighter dunes can be seen filling in relative topographic lows between the blocks (Figure 7). The bright dunes indicate a wind flow from roughly east to west.

[23] Dark mesas within BD are more susceptible to erosion, as evidenced by the formation of dunes in the dark material (Figure 7). Stereo images reveal that the dark mesas are topographically higher standing than the bright blocks, suggesting the dark mesas represent a younger deposit that buried BD and has more recently been eroded to form dunes and expose the underlying BD unit. Dark mesas similar to those seen in BD have also been identified elsewhere in Valles Marineris [*Malin and Edgett*, 2000] and dark mesa-forming units can be seen unconformably overlying brighter, layered outcrops in western Arabia Terra [*Edgett*, 2002].

#### 3.2.2. Sand Dunes (SD) and Sand Sheets (SS)

[24] The contact between the darker unit composed of sand dunes, SD, and BD provides insight into the relative ages of the two units (Figure 8). Blocks from unit BD are visible only in erosional surfaces along the dark unit.

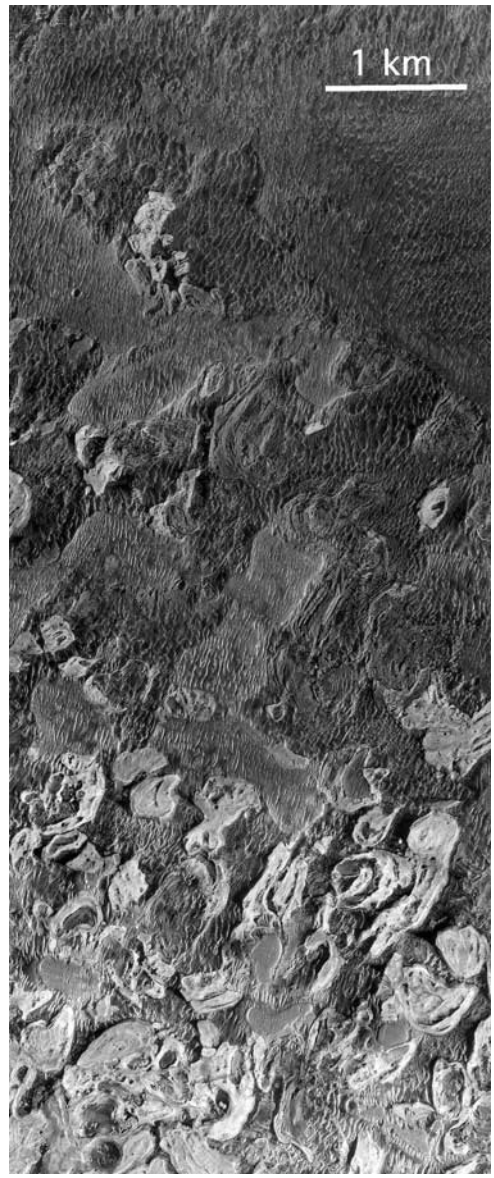


**Figure 8.** Contact between unit BD (bottom) and SD (top). Blocks in BD are partially visible buried by SD and in outliers where erosion of SD has exposed underlying blocks. We propose that SD buried BD and later erosion of SD caused exhumation and exposure of BD. Unit SD is eroding to form sand dunes and ridge-like morphology. In contrast, the blocks of BD appear more competent and less susceptible to this same erosion process. Subframe of MOC image E1203156, which is 3.4 km across.

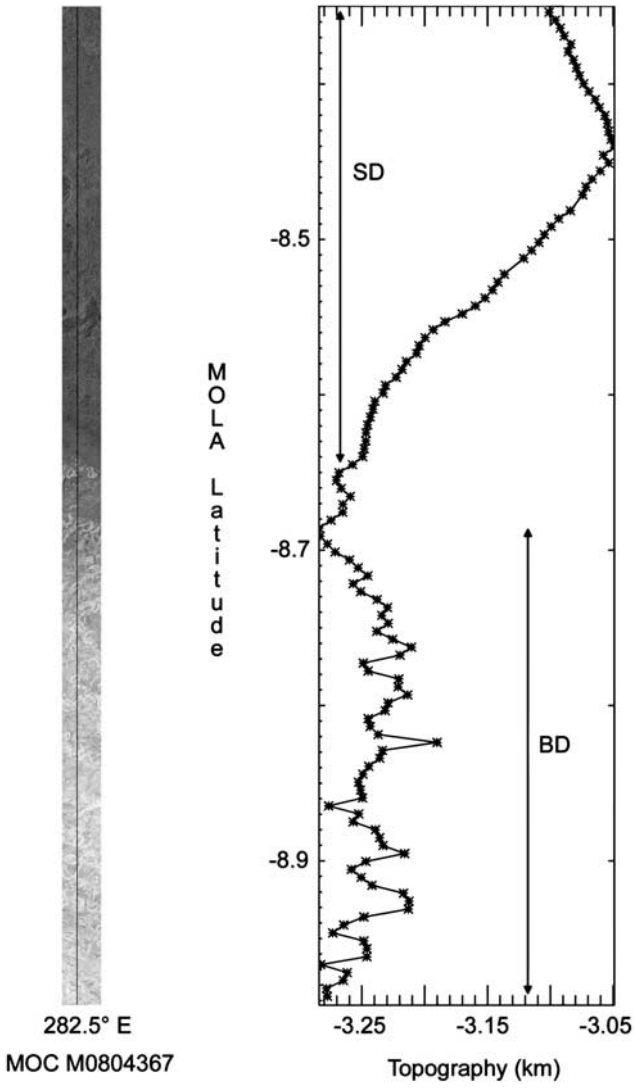


**Figure 9.** MOC image M0804367 and corresponding MOLA profile. The lower half of the MOC image is unit BD and the upper half is unit SD. Unit BD shows 90 meters of topographic variation and has more small-scale roughness and slopes than SD. Unit SD is relatively higher in topography than BD, about 180 meters for this MOLA profile.

Because BD cannot be seen superimposed on the flat-topped dark surfaces, we propose that BD underlies SD and is only being exposed by exhumation. Further support for this interpretation comes from MOLA data which show that the dark unit and dunes to the north of BD are topographically higher (Figure 9). The pieces of dark mesa-forming units visible in BD may be remnants of what had been a spatially larger unit SD that has more recently been eroded, particularly in southwestern Melas Chasma where unit BD is exposed. Consequently, it is possible that BD may extend to much greater areas on the floor but we cannot see it due to burial beneath unit SD. $BD_3$ also appears to be buried beneath SD, particularly to the north where $BD_3$ is visible in a topographic low that appears to be where SD is being eroded away (Figure 4a).

[25] Sand dunes of unit SD appear to be the result of erosion of the dark substrate. Viking and MOC context images suggest dark dunes cover significant amounts of the Melas and Ius Chasma floors, extending far to the east over much of the floor of Melas (Figure 3). Other troughs within Valles Marineris and flat surfaces of ILDs are covered by similar dark dunes and dark mesa-forming units. Although sand dunes are recognizable in much of the unit, the linearity and sharp edges associated with some of the dunes suggest that in fact they could be ridges formed by erosion of an indurated unit. Consequently, we propose that unit SD likely began as aeolian or volcanic airfall that was deposited on all surfaces of Valles Marineris. Later some cementing agent enabled the particles to adhere and form an indurated surface. Wind then eroded this dark unit to produce sand-size debris that eventually formed the sand dunes associated with the unit. At other locales within the unit, wind and desiccation produced the ridges. Remnant outcrops make up the dark mesas visible in BD and elsewhere. The numerous debris aprons that can be seen along steeper edges of ILDs covered with unit SD [*Weitz et al.*, 2001b] attest to the erosion and transport of this dark debris. Unit SD either cannot be more indurated than BD or it must be covered by some dust in order to explain its lower thermal inertia compared to BD.

[26] A dark sand sheet (SS) is located in the west of the ellipse, along the edge of a steep wallrock outcrop. One possibility is that the wallrock represents a topographic barrier that enabled wind to deposit dark debris here but was unable to transport debris up the canyon walls. Irregular, km-size ripples inside the sand sheet appear to form from wind movement east to west around the wallrock. As noted by *Pelkey and Jakosky* [2003], aeolian activity has clearly played an active role in shaping the current surface at the Melas site.

#### 3.2.3. Landslides (LS) and Hummocky Floor Material (HF)

[27] Examination of the canyon walls and floor in the Melas region reveals much evidence for slope failure processes that appear to have occurred throughout the formation of Valles Marineris. These range in scale from large-scale failures on the walls $>100 \times 10^6$ m$^3$ to discrete talus chutes and aprons $<10^6$ m$^3$. Styles of landslide activity at Melas as exemplified on the north canyon wall, may cover the spectrum of complex, composite, successive, multiple, and single. Complex landslides display at least two types of movement (e.g., falling and sliding) in sequence. A composite landslide displays at least two types of movement simultaneously in different parts of the displaced mass. A successive landslide is similar in type to a nearby, earlier landslide, but does not share either displaced material or a rupture surface. Multiple landslides show repeated development of the same type of movement. Finally, a single landslide is a single movement of material.

[28] The hummocky floor unit that we have mapped (HF) may in fact represent landslide material that we cannot trace back to headscarps in the wallrock. The hummocky nature of the unit is similar to that seen in the landslides. Obscuration beneath the sandsheet (SS) also makes it difficult to conclusively link the hummocky floor unit to a possible landslide origin.

[29] The landslides LS, $LS_1$, and $LS_3$ mapped in Figure 3 form part of massive landslide complex. Deposits forming

LS have steep arcuate headscarps, immediately below which are thick deposits of failed material distinguishable by large-scale surface structures that are oriented perpendicular to the downslope direction. Such features are indicative of large-scale tension cracks and the downward sliding of a rock mass occurring dominantly on surfaces of rupture or thin zones of intense shear strain [*Dikau et al.*, 1996]. The failures forming LS were likely deep-seated and sliding may have been translational or had a rotational component. Sliding velocities likely transitioned from long periods of creep (mm/yr) to short periods of acceleration (cm to m/day) ending in catastrophic failure [*Petley et al.*, 2002].

[30] Beyond the slump units in the northwest, one or more thinner aprons of material $LS_1$ and $LS_3$ extend out across the canyon floor. These appear to be reactivation of the slump deposits from LS and aprons can be traced back to several discrete backscarps. The stratigraphic relations of these aprons indicate that runout paths from different sources overlapped and suggests that styles of landslide activity on the north canyon wall were either complex or composite exhibiting at least two types of movement in sequence, or simultaneously in different parts of the displacing mass, respectively. $LS_2$ appears to have originated from a different source than LS, $LS_1$, and $LS_3$. The aprons $LS_1$, $LS_2$, and $LS_3$ have similar characteristics with runouts >10 km, longitudinal grooves, and lobate toes. They are ~60 m thick and ran out over gentle slopes (<5°). Their morphologies and dimensions make them similar to other Martian landslides [*Lucchitta*, 1979, 1987; *Shaller*, 1991] and are analogous to terrestrial rock avalanches [*Voight and Pariseau*, 1978]. The landslides LS, $LS_1$, and $LS_3$ were emplaced as separate events but the time interval between them is unknown. Interpretation is further complicated by the fact that large volume failures usually change behavior between initiation and final deposition. A translational slide may change wholly or in part into a rock avalanche and then into a debris flow. In the case of submarine failures, debris flows can transition to turbidity currents [*Locat and Lee*, 2002].

[31] The blocky deposits do not appear morphologically similar to these other landslides but are proposed to be similar in origin. Unit BD contains rounded, bright blocks with visible layering and albedo differences, in contrast to the more homogeneous nature of the landslides $LS_1$, $LS_2$ and $LS_3$. Because there is no evidence for BD superimposed on or having been deflected around $LS_3$, superposition relations indicate that unit BD lies below $LS_3$, and is thus older. However, the contact between the two units is partially buried beneath sand dunes, making this age relationship difficult to establish. Unit $BD_2$ also appears to lie below $LS_3$ in the THEMIS nighttime infrared image, but without higher resolution MOC images we cannot be certain of the relative ages here either.

#### 3.2.4. Interior Layered Deposit (ILD) and ILD Mensa (IM)

[32] A portion of a larger ILD unit is visible in the southeast of Figure 3. The ILD has numerous layers visible along its slopes, as well as terraces and fluting characteristic of the ILD units in Valles Marineris (see Figure 1a). MOC and THEMIS visible images reveal dark debris covers much of the unit, and dark debris aprons are visible along the steeper slopes. The flat upper surface of the unit has a similar appearance to unit SD, suggesting that the same dark material has been deposited both on the floor of the canyon and on top of the ILD.

[33] To the northeast of the ellipse is a topographic hill that we have mapped as a possible interior layered deposit mound or mensa, IM (Figure 3). The mensa rises approximately 1 km above the surrounding floor. Although no layers are visible in the three MOC narrow angle images of this unit, the topography and morphology of its surface is similar to other ILDs seen within Valles Marineris, including the ILD unit in the southeast that does have visible layering. IM also appears to be covered by a surficial unit with properties similar to those of unit SD and those seen on top of ILD.

#### 3.2.5. Wallrock and Valleys

[34] Most of the wallrock around the Melas site has the typical spur and gully morphology seen elsewhere in Valles Marineris (Figure 1b). However, there exists a surface that has been modified or eroded by fluvial activity along the southern wallrock of Melas, just south of the ellipse. Here we have identified large valleys in the Viking and THEMIS images (see Figure 4b), and even smaller valleys in the MOC narrow angle images (Figure 10c). The valleys in Figure 10c are a few hundred meters long, well-integrated, possess a relatively high drainage density with respect to most Martian systems, increase in width downstream, and head along local ridges. In addition, the valleys do not display many of the prominent features commonly associated with many of the stubby systems (e.g., theater-headed with high depth-length-ratios) flanking Valles Marineris and often attributed to formation by sapping. Moreover, the tendency to head near, and increase in scale away from, divides and their occurrence throughout these localized basins implies a surface source for the water. There is no obvious connection between the large valleys seen in the THEMIS images and the smaller valleys seen in the MOC images.

[35] Also visible in the MOC images are bright deposits perched along the canyon walls. The small valleys cut through both the wallrock and into the brighter units. The contact between these units is often steep and suggests the wallrock unit is fairly competent. Hence stream power that is sufficient for incisement along the trunk valleys may be more limited along lesser, first-order reaches. MOLA profiles along these MOC images reveal that the brighter units correspond to topographic lows along the wallrock (Figures 10a and 10b). No layers are visible within this unit and it appears relatively thin (~few meters). The bright units could be sediments or evaporates that have been superimposed on the eroded wallrock by water flowing in the valleys. Alternatively, they may occur within the wallrock itself and are being exposed over time. Because there are dark-floored valleys that cut through the wallrock but have no associated bright deposits, and there are bright units along the wallrock with no associated valleys, we propose that the bright unit lies within the wallrock and is being exhumed.

[36] Why this bright deposit appears to be concentrated along the southern Melas wallrock in an area with numerous valleys, and how it formed is unclear. The southern wallrock at this location appears as a perched surface about 1 km above the canyon floor (see Figure 2). The typical spur and gully morphology of the wallrock is not visible along this surface but it is seen as small outcrops in the north at the

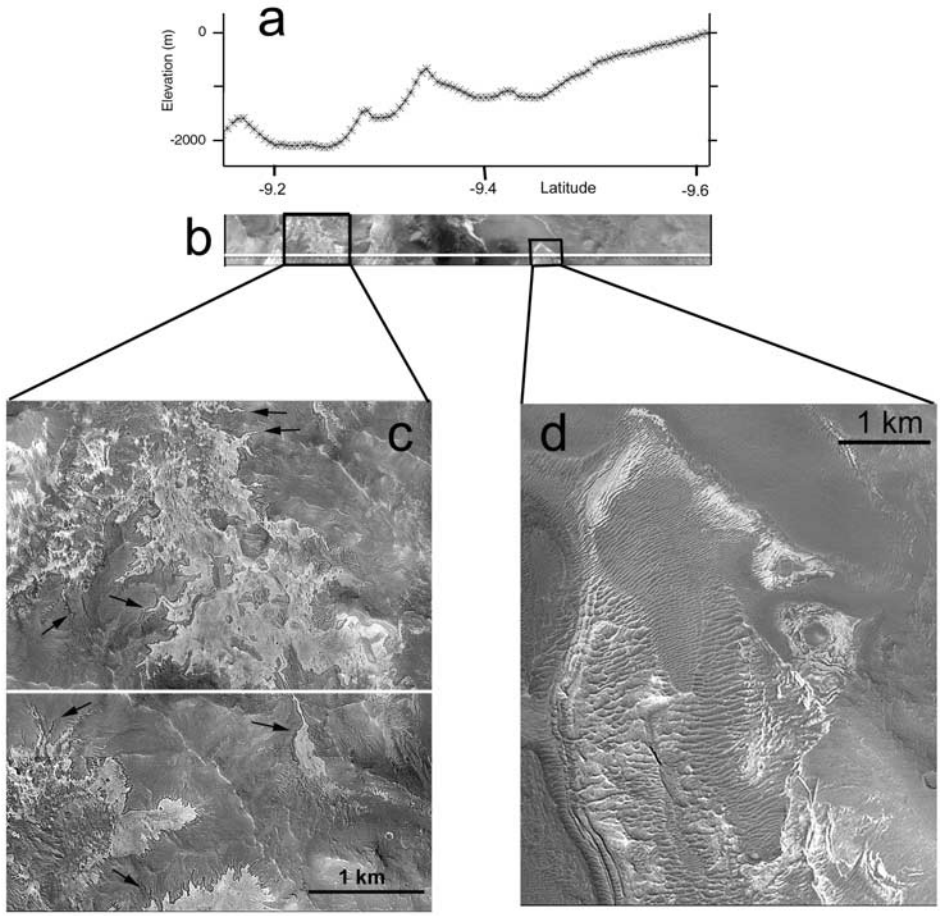


**Figure 10.** (a) MOLA profile and (b) corresponding subframe of MOC image M0702655 along the southern Melas wallrock. White line in the image is the location of the MOLA profile. (c) Enlargement shows a mosaic of MOC images M0702655 and M2301183 with the white line corresponding to the location of MOLA profile. The image reveals numerous small valleys flowing along the southern wallrock of Melas Chasma (black arrows). These valleys are much smaller than the valleys seen in the THEMIS thermal infrared images (see Figure 4b). The brighter unit in the darker wallrock could represent either material carried by water in the valleys and subsequently deposited on the wallrock, or the unit could reside within the wallrock and is being exposed as the wallrock erodes. The topography indicates that the small valleys and bright unit are concentrated in relatively low regions along the wallrock. (d) Brighter, layered deposits further up along the canyon walls that may represent material similar to the source unit for BD.

contact with the canyon floor. The concentration of valleys along the southern Melas wallrock appears to indicate that a source of water existed below the surface of the plateau and produced the valleys after intersecting the edge of the exposed canyon wall. The evidence that the valleys incise into the wallrock suggests that this water flow was long-lived to have produced narrow valleys along several kilometers of wallrock exposure. The relatively young age of the valleys also is an important finding in that it shows water was able to flow in an equatorial region of Mars in perhaps the Late Hesperian to Amazonian.

## 4. Origins for the Blocky Deposit

[37] Two possible explanations for the origin of the blocks in the blocky deposits include the following: (1) they were deposited in situ, such as sedimentary units from air, water, or from volcanic activity, or (2) they are mass movement deposits composed of blocks of layered sedimentary material along the wallrock, but not the wallrock itself. *Komatsu and Cencio* [2002] proposed that the unit could represent an exhumed ILD deposit similar to the larger ILDs found elsewhere in Valles Marineris. However, no ILD units have similar rounded blocks nor would exhumation by the wind explain their rounded, distorted shapes. In addition, the location of all three blocky deposits adjacent to and superimposed on wallrock suggests a correlation between the wallrock and blocky deposits. In the case of $BD_2$ and $BD_3$, the deposits slope downward from north to south, which suggests movement from the wallrock onto the canyon floor. Consequently, in the absence of being able to provide supportive evidence for other origins, we explore the possibility that the blocks were transported as part of a much larger mass wasting flow.

[38] Figure 3 identifies two possible locations for the source of unit BD, assuming it was deposited as a result of mass movement. Originally we proposed [*Weitz et al.*, 2002] that the source for BD was located along the southern wallrock (Figure 3, arrow a). An alternative proposed source for BD [*Skilling et al.*, 2002] is the ILD unit to the southeast (Figure 3, arrow b). *Skilling et al.* [2002] suggest that the steep cliffs along the ILD here could have been the source for a large rock/debris avalanche. If the source is the ILD to the southeast, then the flow would be almost 200 km in length instead of the 60 km that we have mapped. However, there is no indication that BD extends to the southeast. Although MOC narrow angle coverage does not exist to the southeast, MOC context images and THEMIS visible and infrared data do cover this region and neither data set shows the unit extending to this location. It is possible that dunes may obscure the blocky deposit to the southeast, however. Another reason why we do not favor this location for the source of BD is that the avalanche would have had to travel uphill several hundred of meters and through a narrow 15-km valley between the wallrock and ILD before continuing another ~150 km to the current western edge of unit BD.

[39] Several observations support an origin for BD from the southern wallrock. Unit BD can be traced directly to mass wasting seen along the southern Melas wallrock (Figure 11). There are brighter layered deposits along this wallrock above the valleys (see Figure 10d). This layered unit does not appear similar in morphology to the adjacent wallrock and shares more characteristics with ILDs. Whether the layered unit represents the same ILDs as those seen along the canyons floors remains uncertain. Although there is no evidence for mass wasting from this particular unit, similar layered deposits that may exist elsewhere along the southern wallrock could be potential sources for the layered blocks within BD. A more precise location along the wallrock for the actual source of BD cannot be ascertained with the current data sets, however. Both $BD_2$ and $BD_3$ have sources in the canyon walls to the north where there are numerous escarpments, though there are no bright layered deposits that can be identified in the Viking images of these locations. It is unlikely that IM could be the source for $BD_3$ because $BD_3$ can be traced to 1 km elevation up along the canyon walls, which would make it improbable for any single flow to move both to the north up along the wallrock and also to the west along the floor. Units BD and $BD_2$ are distinct units, and consequently have distinct sources, because a topographic ridge extends from the southwest of IM and spatially separates the two units.

[40] If BD, $BD_2$, and $BD_3$ are of mass wasting origin, their distinct morphology when compared to other LS deposits requires explanation. The morphology of a landslide is affected by the starting material, bulk rheology, emplacement dynamics, the environmental conditions under which it formed, and the terrain over which it travels. Landslides containing blocks comparable in size to those in BD occur on Earth on both subaerial [e.g., *Harrison and Falcon*, 1937] and submarine landslides [e.g., *Moore et al.*, 1989; *Watts and Masson*, 1995] and have also been identified on Venus [e.g., *Bulmer and Guest*, 1996; *Bulmer and Wilson*, 1999]. Landslides can be triggered by many causes, including seismic loading [*Keefer*, 1984], volcanic activity [*Kimura and Yamaguchi*, 2000], heavy rainfall, oversteepening, rapid material accumulation and underconsolidation, seepage and glacial loading. Some causes are unique to the marine environment such as gas charging [*Locat and Lee*, 2002]. On Mars, impact craters provide an additional trigger. In addition to occurring in diverse environments, landslides involve volcanic materials [e.g., *Eppler et al.*, 1987], sedimentary materials [*Harrison and Falcon*, 1937], ice [*Heim*, 1932] and where there has been an ice or snow substrate [*Shreve*, 1966]. Unit BD appears to involve layered materials either volcanic or sedimentary in origin. How a landslide behaves between initiation and emplacement depends upon the type of mixture of constituents. On the basis of this, the governing principles


**Figure 11.** Image showing mass wasting along the southern wallrock and onto the canyon floor, with the arrow indicating direction of flow downslope. Unit BD may have originated from this mass wasting event or similar events elsewhere along the wallrock. Subframe of MOC image M2300698.

will either be rock mechanics, fluid mechanics, or torrential hydraulics.

[41] *Lucchitta* [1978, 1979] initially compared large landslides on Mars with dry-runout slides on Earth but subsequently interpreted the morphologies of many to represent mudflow deposits, emplaced in water-saturated conditions [*Lucchitta*, 1987]. *McEwen* [1989] used velocity data from overtopped obstacles, estimated yield strength from thickness and slope values, and log volume versus H/L (H is fall height from top of landslide scarp; L is runout) to counter the idea of large landslides being water saturated. He proposed that the quantitative results showed that large Martian landslides were more analogous to dry slides on Earth. *Shaller* [1991] evaluated the arguments of both *Lucchitta* [1987] and *McEwen* [1989] using terrestrial field data and determined that contrary to the conclusions of *McEwen* [1989], the quantitative measures used failed to distinguish dry from moist or water-saturated landslides. Hence, on the basis of analysis of Viking data it appears that neither landslide morphology nor dimensional data alone can provide definitive insight into their emplacement mechanisms on Mars.

[42] Using MGS data, we have been able to improve dimensional data for landslides in Melas over that from Viking data analyses. The landslides in the Melas region have been compared with a larger more comprehensive data set for landslides [*Bulmer*, 1994] than was available to previous workers. To first-order, landslides on Mars are larger than terrestrial landslides with the exception of those on the seafloor which can have run-out distances in excess of 100 km. Volume appears to override any effects of compositional differences [*Shaller*, 1991]. Another factor of importance appears to be the emplacement environment since comparably large volume landslides on Earth, Mars, and Venus have low but variable values for the coefficient of friction, H/L. Submarine landslides can travel further than those on land, and those on Venus were emplaced in ambient pressures comparable to those on the seafloor [*Bulmer*, 1994]. Unit BD has H/L values from 0.015 to 0.05, assuming H ranges from 1.5 to 3.0 km and L ranges from 60 to 200 km using the two proposed source regions (see Figure 3). This indicates that the resistance to the movement of material was low and that there was an assisting factor enabling long run-out.

[43] Based upon our studies, we propose the possibility that BD may have either been emplaced in a subaqueous environment or that the source material contained some water. In the first scenario, the blocks could have been transported as part of a larger landslide similar to the Alika and Nuuanu submarine landslides on Earth, which have H/L values of 0.02 to 0.06 [*Moore et al.*, 1989]. Submarine landslides also contain blocks similar to those in BD, though not as rounded in morphology. In the second proposed mechanism, if the source material were under water in a lake that once filled Melas Chasma [e.g., *Nedell et al.*, 1987], then rapid removal of this water by drainage to the east along Coprates Chasma and through the outflow channels would create instability along the canyon walls and cause the wet sediments to slump down the wallrock. Slumping of sediments that were still wet could explain the rounded edges of the blocks as they were abraded and carried along the top of the landslide, or as they relaxed and flattened after the slide came to rest. There are several problems with both scenarios, however, including why the blocky deposits only form along the northern and southern wallrocks of Melas Chasma and not elsewhere in Valles Marineris. Hence validation of these two proposed mechanisms may require future data sets, particularly from a lander mission. The other two blocky deposits, $BD_2$ and $BD_3$, would have formed by similar mechanisms, though the limited MOC narrow angle coverage at these two locations makes their origin by these two mechanisms even more speculative.

## 5. Why Melas Would Make a Good Landing Site

[44] The Melas Chasma site was considered a high priority site for MER because of the potential to land on and analyze layered deposits on Mars. The site also would have been publicly engaging because it is located within Valles Marineris, a canyon system that would have provided scenic vistas of the canyon walls. The Athena Science payload [*Squyres et al.*, 2003] has several instruments that would have been valuable to test important scientific hypotheses concerning the composition and formation of layered deposits. For example, Mini-TES, APXS, and Mossbauer could have been used together to identify elements and minerals in the layered blocks of unit BD that would be characteristic of a lacustrine origin, such as clays, salts, carbonates, and sulfides. Alternatively, these data sets may have found basaltic or andesitic compositions that would support a volcanic origin, or at least have suggested that the deposits were basaltic sediments. The Microscopic Imager could also have been used to see textures and the distribution of particle sizes in the layers that would support a particular mode of origin for unit BD. As an example, if the Microscopic Imager identified large particles (>100 microns) in BD, this observation could be used to rule out an aeolian or ashfall origin for the deposits since the particles would be too large to be carried and deposited by suspension in the atmosphere.

[45] Coarse-grained, glassy material, pillow lavas, and welding are all features that can be identified using the Pancam and Microscopic Imager in support of a volcanic origin, such as pyroclastic deposits or tuyas. Aeolian cross-bedding, ripple marks, stratigraphy, bedforms, and any soft sediment deformation features visible in BD as imaged by Pancam could distinguish between an aeolian, volcanic, or lacustrine origin. Pancam images may also reveal striations and flow lobes that would support a mass wasting origin for BD. In summary, numerous tests with the Athena payload could have been applied based upon our proposed origins for BD.

[46] Because of the supporting evidence for water activity in western Melas, this site is compelling from a scientific standpoint for understanding aqueous processes. Although not selected as a MER landing site, this area remains an intriguing site that should be considered for future missions. The safety concerns for the MER EDL landing system limits the site to spacecraft with precision landing and rocket descent. Even with these spacecraft enhancements, there is no guarantee that the landing would be on a layered deposit given the limited number of layers visible in the MOC images of unit BD. The high percentage of dunes

surrounding each block also would still be a cause for concern unless the rover was capable of traversing several kilometers over the course of the mission to guarantee access to the layered blocks. Higher resolution images (~30 cm/pixel) to be acquired from the HiRISE camera on the Mars Reconnaissance Orbiter mission set for launch in 2005 could enhance both our understanding of the formation of unit BD and our ability to identify promising sites in BD for future landers.

## 6. Conclusions

[47] Through detailed morphological studies of the Melas Chasma landing site and associated region, we are able to draw the following conclusions:

[48] (1) The blocky deposits (BD, $BD_2$, and $BD_3$) are most likely mass wasting deposits rather than deposits formed in situ or by other processes.

[49] (2) The source for BD is likely located along the southern wallrock where brighter, layered units have been identified. The process that formed these layered deposits along the canyon walls remains unknown, but their origin could be similar to those postulated for the ILDs. Escarpments along the northern wallrock are the most plausible sources for $BD_2$ and $BD_3$.

[50] (3) BD and $BD_3$ appear to be relatively older deposits that were covered by darker debris of unit SD, which is now eroding to expose the underlying blocky deposits. High thermal inertias, few impact craters, relatively clean surfaces in the MOC images, and exposure of blocks inside weathered portions of SD all support burial and exhumation of BD and $BD_3$.

[51] (4) The distinct morphology of BD, $BD_2$, and $BD_3$ from other landslides in Valles Marineris may be due to different mechanical properties and possibly subaqeuous mass wasting when a lake was present inside Melas Chasma or by collapse and slumping of relatively wet sediments after rapid removal of this lake.

[52] (5) The large number of valleys along the southern Melas Chasma wallrock suggests relatively recent aqueous activity, possibly from an underground water source that intersected the canyon wall exposure and flowed down the wallrock to form valleys.

[53] (6) The Melas site represented the best opportunity for MER to land on possible sedimentary layered deposits inside the Valles Marineris system. Hopefully another future spacecraft will attempt to land and perform scientific analyses at this exciting location.

[54] **Acknowledgments.** This material is based upon work supported by the National Aeronautics and Space Administration under Grant No. NAG5-12306 [CMW] and NAG5-12271 [MHB] issued through the Mars Data Analysis Program. We thank the MER Project for their detailed analyses of the Melas site and the community who attended the MER Landing Site Workshops and provided feedback on the sites, including Melas. An anonymous reviewer and Martha Gilmore provided valuable comments that greatly improved the quality of this paper.

## References

Anderson, F. S., and R. E. Grimm, Rift processes at the Valles Marineris, Mars: Constraints from gravity on necking and rate-dependent strength evolution, *J. Geophys. Res.*, *103*, 11,113–11,124, 1998.

Anderson, F., A. F. C. Haldemann, N. Bridges, M. Golombek, and G. Neumann, Analysis of MOLA data for the Mars Exploration Rover landing sites, *J. Geophys. Res.*, *108*(E12), 8084, doi:10.1029/2003JE002125, in press, 2003.

Arvidson, R. E., F. P. Seelos, K. S. Deal, W. C. Koeppen, N. O. Snider, J. M. Kieniewicz, B. M. Hynek, M. T. Mellon, and J. B. Garvin, Mantled and exhumed terrains in Terra Meridiani, Mars, *J. Geophys. Res.*, *108*(E12), 8073, doi:10.1029/2002JE001982, in press, 2003.

Banerdt, W. B., M. P. Golombek, and K. L. Tanaka, Stress and tectonics on Mars, in *Mars*, edited by H. H. Kieffer et al., pp. 249–297, Univ. of Ariz. Press, Tucson, 1992.

Blasius, K. R., J. A. Cutts, J. E. Guest, and H. Masursky, Geology of the Valles Marineris: First analysis of imaging from the Viking 1 Orbiter primary mission, *J. Geophys. Res.*, *82*, 4067–4091, 1977.

Bulmer, M. H., Small volcanoes in the plains of Venus; with particular reference to the evolution of domes, Ph.D. thesis, 430 pp., Univ. of London, Senate House, London, UK, 1994.

Bulmer, M. H., and J. E. Guest, Modified volcanic domes and associated debris aprons on Venus, in *Volcano Instability*, edited by W. J. McGuire, A. P. Jones, and J. Neuberg, *Geol. Soc. Spec. Publ.*, *110*, 349–371, 1996.

Bulmer, M. H., and J. B. Wilson, Comparison of stellate volcanoes on Earth's seafloor with stellate domes on Venus using side scan sonar and Magellan synthetic aperture radar, *Earth Planet. Sci. Lett.*, *171*, 277–287, 1999.

Bulmer, M. H., O. S. Barnouin-Jha, M. N. Peitersen, and M. Bourke, An empirical approach to studying debris flows: Implications for planetary modeling studies, *J. Geophys. Res.*, *107*(E5), 5033, doi:10.1029/2001JE001531, 2002.

Bulmer, M. H., L. Glaze, K. M. Shockey, O. S. Barnouin-Jha, and W. Murphy, Insights into the emplacement of rock avalanches on Mars, *Lunar Planet. Sci.* [CD-ROM], *XXXIV*, abstract 1225, 2003.

Caruso, P. A., and R. A. Schultz, Slope stability and candidate lithologies of layered wallrock in Valles Marineris, Mars, *Eos Trans. AGU*, *81*(48), Fall Meet. Suppl., abstract P62-08, 2000.

Chapman, M. G., Layered material of variable albedo on Mars: Possible Late Noachian to early Amazonian tephra, *Lunar Planet. Sci.* [CD-ROM], *XXXII*, abstract 1709, 2001.

Chapman, M. G., and B. K. Lucchitta, New Mars data suggest Melas Chasma interior deposits are sub-ice volcanoes, paper presented at Geological Society of America Annual Meeting, Geol. Soc. of Am., Reno, Nev., 2000.

Chapman, M. G., and K. L. Tanaka, Interior trough deposits on Mars: Subice volcanoes?, *J. Geophys. Res.*, *106*, 10,087–10,100, 2001.

Christensen, P. R., et al., Detection of crystalline hematite mineralization on Mars by the Thermal Emission Spectrometer: Evidence for near-surface water, *J. Geophys. Res.*, *105*, 9623–9642, 2000.

Dikau, R., D. Brunsden, L. Schrott, and M-L. Ibsen (Eds.), *Landslide Recognition: Identification, Movement and Causes*, 251 pp., John Wiley, Hoboken, N. J., 1996.

Edgett, K. S., Low-albedo surfaces and eolian sediment: Mars Orbiter Camera views of western Arabia Terra craters and wind streaks, *J. Geophys. Res.*, *107*(E6), 5038, doi:10.1029/2001JE001587, 2002.

Eppler, D., J. Fink, and R. Fletcher, Rheological properties of emplacement of the Chaos Jumbles rockfall avalanche, Lassen Volcanic National Park, California, *J. Geophys Res.*, *92*, 3623–3633, 1987.

Gaddis, L. R., and T. N. Titus, Valles Marineris, Mars: Mapping basaltic units using TES data, *Lunar Planet. Sci.* [CD-ROM], *XXXI*, abstract 1976, 2000.

Geissler, P. E., R. B. Singer, G. Komatsu, S. Murchie, and J. Mustard, An unusual spectral unit in west Candor Chasma: Evidence for aqueous or hydrothermal alteration in the Martian canyons, *Icarus*, *106*, 380–391, 1993.

Golombek, M. P., et al., Selection of the Mars Exploration Rover landing sites, *J. Geophys. Res.*, *108*(E12), 8072, doi:10.1029/2003JE002074, in press, 2003.

Harrison, J. V., and N. L. Falcon, The Saidmarreh landslip, southwest Iran, *Geogr. J.*, *89*, 42–47, 1937.

Heim, A., *Bergsturz und Menschenleben*, 218 pp., Fretz and Wasmuth A.G., Zurich, 1932.

Kass, D., J. T. Schofield, T. Michaels, S. Rafkin, M. Richardson, and A. Toigo, Analysis of atmospheric mesoscale models for entry, descent, and landing, *J. Geophys. Res.*, *108*(E12), 8090, doi:10.1029/2003JE002065, in press, 2003.

Keefer, D., Landslides caused by earthquakes, *Geol. Soc. Am. Bull.*, *95*, 406–421, 1984.

Kimura, H., and Y. Y. Yamaguchi, Detection of landslide areas using radar interferometry, *Photogramm. Eng. Remote Sens.*, *66*(3), 337–344, 2000.

Kirk, R. L., E. Howington-Kraus, and B. Archinal, Topographic analysis of candidate Mars Exploration Rover landing sites from MOC narrow-angle stereoimages, *Lunar Planet. Sci.* [CD-ROM], *XXXIII*, abstract 1988, 2002.

Komatsu, G., and A. D. Cencio, The origin of light-colored units on the floor of Valles Marineris, Mars, *Lunar Planet. Sci.* [CD-ROM], *XXXIII*, abstract 1184, 2002.

Komatsu, G., P. E. Geissler, R. G. Strom, and R. B. Singer, Stratigraphy and erosional landforms of layered deposits in Valles Marineris, Mars, *J. Geophys. Res.*, *98*, 11,105–11,121, 1993.

Locat, J., and H. J. Lee, Submarine landslides: Advances and challenges, *Can. Geotech. J.*, *39*, 193–212, 2002.

Lucchitta, B. K., A large landslide on Mars, *Geol. Soc. Am. Bull.*, *89*, 1601–1609, 1978.

Lucchitta, B. K., Landslides in the Valles Marineris, Mars, *J. Geophys. Res.*, *84*(B14), 8097–8113, 1979.

Lucchitta, B. K., Valles Marineris Mars: Wet debris flows and ground ice, *Icarus*, *72*, 411–429, 1987.

Lucchitta, B. K., Young volcanic deposits in the Valles Marineris, Mars, *Icarus*, *86*, 476–509, 1990.

Lucchitta, B. K., MOC images confirm the layered deposits formed within Valles Marineris, *Lunar Planet. Sci*. [CD-ROM], *XXXII*, abstract 1359, 2001.

Lucchitta, B. K., and L. M. Bertolini, Interior structures of the Valles Marineris (abstract), *Lunar Planet. Sci.*, *XXI*, 722–723, 1989.

Lucchitta, B. K., A. S. McEwen, G. D. Clow, P. E. Geissler, R. B. Singer, R. A. Schultz, and S. W. Squyres, The canyon system on Mars, in *Mars*, edited by H. H. Kieffer et al., pp. 453–492, Univ. of Ariz. Press, Tucson, 1992.

Lucchitta, B. K., N. K. Isbell, and A. Howington-Kraus, Topography of Valles Marineris: Implications for erosional and structural history, *J. Geophys. Res.*, *99*, 3783–3798, 1994.

Malin, M. C., Nature and origin of the intercrater plains on Mars, Ph.D. thesis, Calif. Inst. of Technol., Pasadena, Calif., 1976.

Malin, M. C., and K. S. Edgett, Sedimentary rocks of early Mars, *Science*, *290*, 1927–1937, 2000.

McCauley, J. F., Geologic map of the Coprates quadrangle of Mars, *U.S. Geol. Surv. Misc. Invest. Ser.*, *Map I-897*, 1978.

McEwen, A. S., Mobility of large rock avalanches: Evidence from Valles Marineris, Mars, *Geology*, *17*, 1111–1114, 1989.

McEwen, A. S., M. C. Malin, M. H. Carr, and W. K. Hartmann, Voluminous volcanism on early Mars revealed in Valles Marineris, *Nature*, *397*, 584–586, 1999.

Mège, D., and P. Masson, Amounts of crustal stretching in Valles Marineris, Mars, *Planet. Space Sci.*, *44*, 749–782, 1996a.

Mège, D., and P. Masson, A plume tectonics model for the Tharsis province, Mars, *Planet. Space Sci.*, *44*, 1499–1546, 1996b.

Mellon, M. T., B. M. Jakosky, H. H. Kieffer, and P. R. Christensen, High-resolution thermal inertia mapping from the Mars Global Surveyor Thermal Emission Spectrometer, *Lunar Planet. Sci.* [CD-ROM], *XXXI*, abstract 1898, 2000.

Moore, J. G., D. A. Clague, R. T. Holcomb, P. W. Lipman, W. R. Normark, and M. E. Torresan, Prodigious submarine landslides on the Hawaiian ridge, *J. Geophys. Res.*, *94*, 17,465–17,484, 1989.

Murchie, S. L., S. Erard, J. F. Mustard, J. P. Bibring, Y. Langevin, J. W. Head, and C. M. Pieters, The geology of the interior deposits of Valles Marineris from Viking images and ISM imaging spectroscopy, *Lunar Planet. Sci.*, *XXIII*, 945–946, 1992.

Murchie, S. L., L. Kirkland, S. Erard, J. Mustard, and M. Robinson, Near-Infrared spectral variations of Martian surface materials from ISM imaging spectrometer data, *Icarus*, *147*, 444–471, 2000.

Nedell, S. S., S. W. Squyres, and D. W. Anderson, Origin and evolution of the layered deposits in the Valles Marineris, Mars, *Icarus*, *70*, 409–441, 1987.

Pelkey, S. M., and B. M. Jakosky, Geologic surveys of Gale Crater and Melas Chasma, Mars: Integration of remote sensing data, *Icarus*, in press, 2003.

Peterson, C., A secondary origin for the central plateau of Hebes Chasma, *Proc. Lunar Planet. Sci. 11th*, 1459–1471, 1981.

Petley, D., M. H. Bulmer, and W. Murphy, Patterns of movement of rotational and translational landslides, *Geology*, *30*(8), 719–722, 2002.

Peulvast, J. P., and P. L. Masson, Melas Chasma: Erosion and tectonics in central Valles Marineris (Mars): A new morpho-structural model, *Earth Moon Planets*, *61*, 191–217, 1993a.

Peulvast, J. P., and P. L. Masson, Melas Chasma: Morphology and tectonic patterns in central Valles Marineris, *Earth Moon Planets*, *61*, 219–248, 1993b.

Rafkin, S., and T. Michaels, Meteorological predictions for 2003 Mars Exploration Rover landing sites, *J. Geophys. Res.*, *108*(E12), 8091, doi:10.1029/2002JE002027, in press, 2003.

Schultz, R. A., Complex early rifting in Valles Marineris: Results from preliminary geologic mapping of the Ophir Planum region of Mars, 1:50,0000 scale (abstract), *Lunar Planet. Sci.*, *XXI*, 1103–1104, 1990.

Schultz, R. A., Structural development of Coprates Chasma and western Ophir Planum, Valles Marineris rift, Mars, *J. Geophys. Res.*, *96*, 22,777–22,792, 1991.

Schultz, R. A., Gradients in extension and strain at Valles Marineris, Mars, *Planet. Space Sci.*, *43*, 1561–1566, 1995.

Schultz, R. A., Dual-process genesis for Valles Marineris basins and troughs on Mars (abstract), *Lunar Planet. Sci.*, *XXVIII*, 1263–1264, 1997.

Shaller, P. J., Analysis and implications of large Martian and terrestrial landslides, Ph.D. thesis, 586 pp., Calif. Inst. of Technol., Pasadena, 1991.

Shreve, R. L., Sherman landslide, Alaska, *Science*, *154*, 1639–1643, 1966.

Skilling, I. P., M. G. Chapman, and B. K. Lucchitta, Young, blocky flows in East Ius/West Melas and West Candor Chasmata, Mars: Debris avalanche deposits derived from interior layered deposit (ild) mounds?, *Lunar Planet. Sci.* [CD-ROM], *XXXIII*, abstract 1361, 2002.

Spencer, J. R., and S. K. Croft, Valles Marineris as karst: Feasibility and implications for Martian atmospheric evolution, in *Reports of Planetary Geology and Geophysics Program-1985*, *NASA Tech. Memo*., *TM-88,383*, 193–195, 1986.

Spencer, J. R., and F. P. Fanale, New models for the origin of Valles Marineris closed depressions, *J. Geophys. Res.*, *95*, 14,301–14,313, 1990.

Squyres, S. W., et al., Athena Mars Rover science investigation, *J. Geophys. Res.*, *108*(E12), 8062, doi:10.1029/2003JE002121, in press, 2003.

Tanaka, K. L., Origin of Valles Marineris and Noctis Labyrinthus, Mars, by structurally controlled collapse and erosion of crustal materials (abstract), *Lunar Planet. Sci.*, *XXVIII*, 1413–1414, 1997.

Tanaka, K. L., and D. J. MacKinnon, Pseudokarst origin for Valles Marineris, *Lunar Planet. Sci*. [CD-ROM], *XXXI*, abstract 1780, 2000.

Toigo, A., and M. Richardson, Meteorology of proposed Mars Exploration Rover landing sites, *J. Geophys. Res.*, *108*(E12), 8092, doi:10.1029/2003JE002064, in press, 2003.

Varnes, D. J., Slope movements and types and processes, in *Landslides: Analysis and Control*, *Spec. Rep. Transp. Res. Board. Natl. Res. Board*, vol. 176, pp. 11–33, Natl. Acad. of Sci., Washington, D. C., 1978.

Voight, B., and W. Pariseau, *Rockslides and Avalanches*, vol. 1, *Natural Phenomena*, *Dev. Geotech. Eng.*, vol. 14A, Elsevier Sci., New York, 1978.

Watts, A. B., and D. G. Masson, A giant submarine slide on the north flank of Tenerife, Canary Islands, *J. Geophys. Res.*, *100*, 24,487–24,498, 1995.

Weitz, C. M., A volcanic origin for the interior layered deposits in Hebes Chasma, Mars, *Lunar Planet. Sci*. [CD-ROM], *XXX*, abstract 1277, 1999.

Weitz, C. M., and T. J. Parker, New evidence that the Valles Marineris interior layered deposits formed in standing bodies of water, *Lunar Planet. Sci*. [CD-ROM], *XXXI*, abstract 1693, 2000.

Weitz, C. M., T. J. Parker, and F. S. Anderson, Potential MER landing site in Melas Chasma, paper presented at First Mars 2003 Landing Site Workshop, Ames Res. Cent., Moffett Field, Calif., 24 –25 Jan. 2001a.

Weitz, C. M., T. J. Parker, F. S. Anderson, and J. A. Grant, The interior layered deposits of Valles Marineris: Layering, erosional processes, and age relationships, *Lunar Planet. Sci*. [CD-ROM], *XXXII*, abstract 1629, 2001b.

Weitz, C. M., T. J. Parker, F. S. Anderson, and J. A. Grant, Geology of a proposed MER landing site in Western Melas Chasma, *Lunar Planet. Sci*. [CD-ROM], *XXXIII*, abstract 1246, 2002.

Witbeck, N. E., K. L. Tanaka, and D. H. Scott, *U.S. Geol. Surv. Misc. Invest. Ser. Map*, *I-2010*, 1991.

Zuber, M. T., et al., Internal structure and early thermal evolution of Mars from Mars Global Surveyor topography and gravity, *Science*, *287*, 1788–1793, 2000.

F. S. Anderson, University of Hawai'i at Manoa, Hawai'i Institute of Geophysics and Planetology, 2525 Correa Road, Post 526B, Honolulu, HI 96822, USA.

M. H. Bulmer, Joint Center for Earth Systems Technology, University of Maryland, Baltimore, MD 21250, USA.

J. A. Grant, Center for Earth and Planetary Studies, National Air and Space Museum, Smithsonian Institution, Independence Avenue at 6th Street SW, Washington, DC 20560, USA.

T. J. Parker, Jet Propulsion Laboratory, 4800 Oak Grove Drive, Pasadena, CA 91109, USA.

C. M. Weitz, Planetary Science Institute, 1700 East Fort Lowell, Suite 106, Tucson, AZ 85719, USA. (cweitz@hq.nasa.gov)